Carbohydrate Polymers 96 (2013) 91–100

Contents lists available at SciVerse ScienceDirect

Carbohydrate Polymers

journal homepage: www.elsevier.com/locate/carbpol

Preparation and properties of blends composed of lignosulfonated layered double hydroxide/plasticized starch and thermoplastics

Edwige Privas[a], Fabrice Leroux[b], Patrick Navard[a,*]

[a] Mines ParisTech, CEMEF – Centre de Mise en Forme des Matériaux, CNRS UMR 7635, Rue Claude Daunesse, CS 10207, 06904 Sophia Antipolis cedex, France[1]

[b] Institut de Chimie de Clermont-Ferrand (ICCF), Université Blaise Pascal, CNRS, UMR 6096, ICCF, F-63177 Aubière, France

ARTICLE INFO

Article history:
Received 16 January 2013
Received in revised form 10 March 2013
Accepted 12 March 2013
Available online 19 March 2013

Keywords:
Layered double hydroxide
Lignosulfonate
Starch
Nanocomposite
Polyethylene
Polymer blend

ABSTRACT

Layered double hydroxide prepared with lignosulfonate (LDH/LS) can be easily dispersed down to the nanometric scale in thermoplastic starch, at concentration of 1 up to 4 wt% of LDH/LS. They can thus be used as a bio-based reinforcing agent of thermoplastic starch. Incorporation of LDH/LS in starch must be done using LDH/LS slurry instead of powder on order to avoid secondary particles aggregation, the water of the paste being used as the starch plasticizer. This reinforced starch was used for preparing a starch–polyolefine composite. LDH/LS–starch nanocomposites were mixed in a random terpolymer of ethylene, butyl acrylate (6%) and maleic anhydride (3%) at concentrations of 20 wt% and 40 wt%. With a 20% loading of (1 wt% LDH/LS in thermoplastic starch), the ternary copolymer is partially bio-based while keeping nearly its original processability and mechanical properties and improving oxygen barrier properties. The use of layered double hydroxides is also removing most odours linked to the lignin phase.

1. Introduction

Starch has been extensively studied as a structural or functional polymer because of its renewability, abundance and biodegradability. A major breakthrough was the discovery of its thermoplasticity when processed with a low content of water or plasticizer, at elevated temperature and under mechanical action (Forssell, Mikkilä, Moates, & Parker, 1997). This opened the way to prepare starch-based polymer blends that are now commercially used for a variety of applications like biodegradable packaging films. During the processing used for preparing thermoplastic starch, the native granular structure of starch is destroyed and amylose and amylopectin are dispersed and more or less randomly distributed in the medium, leading to an amorphous thermoplastic material that can recrystallise with time, but with crystalline structures different from the ones present in native starch granules (Bastioli, 1998; Van Soest & Esser, 1997). However, thermoplastic starch is suffering several drawbacks, the most important ones being its poor mechanical properties and its sensitivity to water (Chaléat, Halley, & Truss, 2008; Follain, Joly, Dole, & Bliard, 2005). When the sensitivity to moisture must be decreased, starch can be embedded in a matrix composed of a hydrophobic polymer. Regarding mechanical properties, brittleness is decreased by the addition of a plasticizer like water or glycerol, but this is degrading its mechanical strength. To improve the low mechanical tensile properties, a classical strategy consists on including soft or rigid small particles. One possibility which has been widely studied is the use of nanosized particles. Such nanocomposites have met a wide range of applications in environmental (i.e. catalytic degradation, detection of contaminants) (Zhao et al., 2011), optical (i.e. OLED, photovoltaic cells) (Nguyen, 2011), biomedical (Armentano, Dottori, Fortunati, Mattioli, & Kenny, 2010) or packaging (Tang, Kumar, Alavi, & Sandeep, 2012) sectors. One advantage of nanocomposites is the low content of fillers (less than 5 wt%) needed to match the properties of conventional composites with much higher loadings. Nanoscale fillers have a much higher surface area than conventional fillers, increasing enormously the interactions between filler and polymer matrix (Chivrac, Kadlecova, Pollet, & Avérous, 2006). Nanocomposites can be used to prepare light composites having large modulus, low permeability, good thermal stability or transparency. Nanofillers have at least one dimension in the nanometric range, like clay, carbon nanotubes, graphene, or cellulose nanowhiskers. Depending of process conditions and affinity between fillers and matrices, different states of dispersion can be obtained: (a) phase separated with aggregates called microcomposite, (b) intercalated where layers are uniformly dispersed but remain ordered and (c) exfoliated when filler is fully and uniformly dispersed and completely disoriented. Exfoliated structures are

* Corresponding author. Tel.: +33 493957466; fax: +33 492389752.
E-mail address: patrick.navard@mines-paristech.fr (P. Navard).

[1] Member of the European Polysaccharide Network of Excellence http://www.epnoe.eu.

0144-8617/$ – see front matter © 2013 Elsevier Ltd. All rights reserved.
http://dx.doi.org/10.1016/j.carbpol.2013.03.042

always the ultimate goal in nanocomposite compounding since the best performances especially concerning barrier properties should be obtained (Vaia & Giannelis, 1997).

Starch filled with nanostructures has been studied in order to improve mechanical stiffness, barrier properties and to reduce flammability. Various types of inorganic layered fillers such as montmorillonite (Park et al., 2002), hectorite (Chen & Evans, 2005), kaolin (Carvalho, Curvelo, & Agnelli, 2001) or layered double hydroxide (Wu, Chang, & Ma, 2011) have been tried. Storage modulus of starch nanocomposites was found to be in the following order, with the best results obtained for kaolinite: kaolinite > brucite > hectorite > layered double hydroxide (Wihelm, Sierakowski, Souza, & Wypych, 2003a). Property improvement is very much dependent on the possibility to obtain a good dispersion of nanofillers and a good interfacial adhesion between fillers and matrix. However, it was reported that clay is difficult to be dispersed in starch (Bagdi, Muller, & Pukanszky, 2006; Chiou et al., 2006; Park, Lee, Park, Cho, & Ha, 2003). It was also reported that glycerol, used as a starch plasticizer, had the tendency to penetrate clay fillers leading to non exfoliated structures (Wihelm, Sierakowski, Souza, & Wypych, 2003b). To improve the dispersion of nanofillers into the starch matrix, the counter anion should be compatible with starch (Chivrac, Pollet, Schmutz, & Avérous, 2008). Pandey and Singh (2005) studied different methods to prepare starch–clay nanocomposites, the best intercalation results being obtained with the incorporation of the plasticizer after mixing starch with clay since polymer chains can then migrate inside the clay galleries before the plasticizer molecules.

Among the family of clay nanofillers, layered double hydroxides (LDH) present the advantage to be highly versatile with many options for choosing the anionic organic interlayer molecules, giving a large variety of LDH hybrid materials (Leroux, 2006). Although LDH can be found in nature, they can also be synthetized to fulfil specific requirement at relatively low cost (Utracki, Sepehr, & Boccaleri, 2007). Layered double hydroxides are based on positively charged brucite-like sheets formed by the substitution of divalent to trivalent cations, leading to a positive charge sheet counterbalanced by the presence of an anion in the interlayer space. A previous study show that it is possible to used a widely available by-product of the pulp industry, lignosulfonate, as the organo-modifying molecule intercalated into layered double hydroxide (Hennous et al., 2013), having in mind that such formed fillers are environmentally-friendly since MgAl-hydrotalcite is typically envisioned for drug delivery (Costantino, Nocchetti, Tammaro, & Vittoria, 2012) and as a gene reservoir (Oh, Park, Choi, & Choy, 2012). Recently reported to organo-modify LDH platelets, alginate (another bio-related polymer) was found to improve the detection sensitivity of sensor-based systems (Sanchez-Paniaguar Lopez, Leroux, & Mousty, 2010) and the ion conductivity for polymer electrolytes (Leroux, Chabrol, Morlat-Thérias, Gardette, & de Roy, 2012). Lignosulfonate are water-soluble anionic polyelectrolyte polymers obtained in large quantities. When not burned, they are mainly used in making concrete for superplasticizing effect, in drilling fluids, and as dispersants in various applications.

The aim of the present study is to study the preparation of layered double hydroxide/lignosulfonate (LDH/LS)-reinforced thermoplastic starch/polyethylene based polymer blends and to evaluate their interest, mainly considering gas barrier and mechanical properties.

2. Experimental

2.1. Materials

Native corn starch was provided by Novamont (Italy). Calcium lignosulfonate was kindly supplied by Tembec (France) as a brown powder with a calcium content of 3% dry matter. Glycerol was an analytical grade purchased from Sigma–Aldrich. Lotader 3210 is a random terpolymer of ethylene, butyl acrylate (6%) and maleic anhydride (3%) produced and kindly given by Arkema (France).

2.2. Preparation of LDH–lignosulfonate (LDH/LS)

LDH composition is Zn_2Al and is prepared by a co-precipitation method as explained in a previous article (Hennous et al., 2013). The prepared LDH/LS mixture was kept in slurry form with 18% dry matter.

2.3. Preparation of LDH/LS–thermoplastic corn starch (TCS)

Corn starch powder was first dried overnight at 70 °C under vacuum to remove the free water (~10 wt% of the material). The content of glycerol was fixed at 35 wt% based on dry starch. Water is used as co-plasticizer in the range of 15 wt%. The filler loading levels of LDH/LS were 0, 1, 2, and 4 wt% based on dry starch. The preparation of the thermoplastic starch mixture with glycerol and LDH/LS was performed in two steps. In the first step, a quantity of LDH/LS mixture was dispersed into glycerol using vigorous magnetic stirring until complete dispersion of LDH/LS. Corn starch was then mixed manually with the obtained plasticizer–nanofiller mixture. In the second step, the total glycerol–starch–LDH/LS–water mixture was sheared in an internal mixer Haake Rheomix 600 equipped with roller rotors at 90 °C and 100 rpm for 20 min. The LDH/LS–plasticized starch blends were injection moulded into tensile test specimens using a MiniJet apparatus from ThermoFisher at 160 °C, with the mould at 50–65 °C and injection pressure of 300–600 bars. Specimens were kept in a conditioning room at 20 °C and 55% relative humidity before characterization. Part of blends was kept as granulates for further blending with the Lotader thermoplastic and the other part was used to prepare test specimens for X-ray scattering were compression moulded into pieces of 50 mm × 50 mm × 2 mm.

2.4. Preparation of Lotader-thermoplastic reinforced with LDH/LS–TCS

LDH/LS–TCS granulates obtained as described previously and Lotader 3210 were dried overnight at 50 °C under vacuum. Lotader/(LDH/LS–TCS) nanocomposites were blended in an internal mixer Haake Rheomix 600 equipped with roller rotors at 140 °C and 100 rpm for 10 min. Loadings of LDH/LS–TCS nanocomposites into Lotader 3210 matrix were 20 and 40 wt%. The blends were then compression moulded and (1) cut as tensile test specimens ISO 527-1BA, or (2) into 20 mm circular specimens of 2 mm thickness for rheology measurements, or (3) cut as test samples of 50 mm × 50 mm × 2 mm for water sensitivity measurement, or (4) formed as 100 mm circular films of 400 μm thickness for O_2 permeability measurements.

2.5. Characterization

2.5.1. Odour and volatile compound analyses

Odour and volatile organic compounds were determined with an electronic nose HERACLES from Alpha M.O.S. (France). HERACLES electronic nose is equipped with two columns (DB5 apolar and DB1701 slightly polar), 2 m length and 100 μm in diameter. Calibration was done with alcane from *n*-hexane to *n*-hexadecane. Data treatment was done with Alphasoft V12.3 software using AroChemBase database. Table 1 gives the parameters of analysis used for lignosulfonate and lignosulfonate interleaved into Zn_2Al layered double hydroxide.

Table 1
Parameters of HERACLES analysis used to study lignosulfonate and lignosulfonate modified LDH.

Incubation	
Sample weight	0.5 g
Incubation temperature	40 °C
Incubation time	20 min
Injection	
Volume	1 mL
Injection temperature	170 °C
Injection time	12 s
Trap	
Type	Tenax®[a]
Trap temperature	250 °C
Chromatography	
Program	40 °C (2 s)–270 °C (2 s) at 5 °C/s
Detector temperature	280 °C
Acquisition time	50 s

[a] Tenax® is a porous polymer resin based on 2,6-diphenylene-oxide.

2.5.2. X-ray diffraction (XRD)

X-ray diffraction measurements were performed on compressed squared specimens with dimension of 50 mm × 50 mm × 2 mm using a Siemens D500 X-ray diffractometer with Cu Kα source. Measurements were performed between 2° and 70° with steps of 0.08° and an acquisition time of 4 s. Crystallinity was determined following Hermans and Weidinger (1949): $X_c = \frac{1}{1+(p/q')(I_a/I_c)}$ with $p/q = 1.297$.

2.5.3. Transmission electron microscopy (TEM) and scanning electron microscopy (SEM)

Morphology observations were performed on a SEM-FEG (Field Emission Gun) ZEISS Supra 40 at acceleration voltage of 3 kV. Before observation, cryofractured Lotader/(LDH/LS–TCS) samples were immersed during 20 min into an acid chloride solution concentrated at 5 N to remove the starch part. Samples were then washed with water and dried overnight at 50 °C. To avoid charge accumulation effects, a thin layer of gold-palladium was deposited by sputtering onto the surface of samples. The SEM micrographs were used to measure the diameter of dispersed phase by an automatic method using the image analyser software Ellix (Microvision). Dispersed object cuts were considered circular and approximated with circles from which diameters were extracted. Note that this method faces the problem of conversion of a two-dimensional distribution into a three-dimensional one, cryofractured not cutting the dispersed phase at the equator. For each sample, three micrographs were used and 70–700 diameter measurements were made.

TEM observations were done on cryomicrotomed surface obtained by cutting an injection bar with an ultracryomicrotome Leica FC7. Observations were done with a Jeol JEM 1400 at 120 kV.

2.5.4. Rheological properties

Dynamic oscillatory rheometer measurements were performed on a strain rate controlled ARES rheometer (TA Instruments) with plate–plate geometry (20 mm diameter, gap = 1.6 mm). TCS, LDH/LS–TCS and Lotader, Lotader/(LDH/LS–TCS) formulations were submitted to time sweep tests at 150 °C in order to evaluate thermal stability and to strain sweep tests to determine the extend of the linear domain. The deformation rate was fixed at 0.1% for TCS and LDH/LS–TCS blends and at 5% for Lotader and Lotader/(LDH/LS–TCS) blends.

2.5.5. Mechanical tests

Tensile strength, Young's modulus and elongation at break were measured according to ISO 527 standard on a Zwick universal testing machine using a load cell of 2 kN and an extensometer. Crosshead speed of 1 mm/min was used for Young's modulus determination and a speed of 5 mm/min after the elastic region. A minimum of three tests were performed for each measurement.

Table 2
Volatile compounds of lignosulfonate identified by Kovats retention index. A is pure lignosulfonate, B is LDH/LS compounds.

Volatile compound	Smell	Ratio
Acetic acid	Vinegar	A ≫ B
Butyric acid/furfural	Cheese	A ≫ B
Carboxylic acid		A ≫ B
2-Heptanol	Mushroom	B > A
2,5-Dimethylpyrazine	Cacao	A > B

2.5.6. Sensitivity to water and oxygen transmission rate (OTR)

Sensitivity to water was measured by a gravimetric method. A sample of dimension 50 mm × 50 mm × 2 mm was dried at 80 °C under vacuum for 48 h and its initial dry weight was measured. The dry sample was then immersed in distilled water at room temperature and its weight was measured at regular time intervals after removing the surface water with paper until, weight stabilization (∼310 h). The diffusion coefficient ($m^2\ s^{-1}$) at short time was calculated with Eq. (1) by plotting $M_t/M_\infty = f(t^{1/2})$ (Dufresne, Dupeyre, & Vignon, 2000).

$$\frac{M_t}{M_\infty} = \frac{4}{l}\left(\frac{D}{\pi}\right)^{1/2} t^{1/2} \quad \text{with} \quad l = \text{half-thickness} \quad (\text{m}) \tag{1}$$

Oxygen transmission rate (in $cm^3/(m^2\ day)$) through the nanocomposite films was measured with a Systech 8700 device. Sample surface area was 19.6 cm^2 (a diameter of 50 mm) with thickness about 400 μm.

3. Results and discussion

3.1. LDH/LS odour characterization

Lignosulfonates as all lignin and most lignin derivatives have a typical strong odour that can be a disadvantage for some applications, in particular if such compounds are placed in a confined, warm environment such as a car in a sunny place. We noticed a very large difference of odour between the used lignosulfonate and its LDH/LS counterpart. After intercalation into layered double hydroxides, the characteristic odour seemed to have nearly disappeared. An electronic nose was used to qualify and quantify such change of odour. Chromatograms obtained for pure lignosulfonate (A) and LDH/LS compound (B) are shown in Fig. 1. Pure lignosulfonate has a higher quantity of volatiles compounds. The major volatiles compounds of lignosulfonate were identified using Kovats retention index (Table 2).

Odour is suppressed due to the synthesis process. During the washing stage of the intercalation process, compounds other than lignosulfonates, including hemicelluloses, are not intercalated and they are left in the washing bath. This cleaning process is strongly reducing the odour of the LDH/LS. The presence of acetic acid and furfural may correspond to traces of the degradation of hemicellulosic components (Peters, Fischer, & Fischer, 2008) which are not kept in the LDH/LS materials, underlining the role of LDH as an efficient sieve towards organic molecule.

3.2. LDH/LS–TCS nanocomposite

3.2.1. Mixing process

Upon mixing, starch plasticization occured in a few together with the simultaneous dispersion and distribution of LDH/LS. Whatever the amount of LDH/LS fillers was, the final torque reached a common value of about 20 Nm and a temperature of about 140 °C.

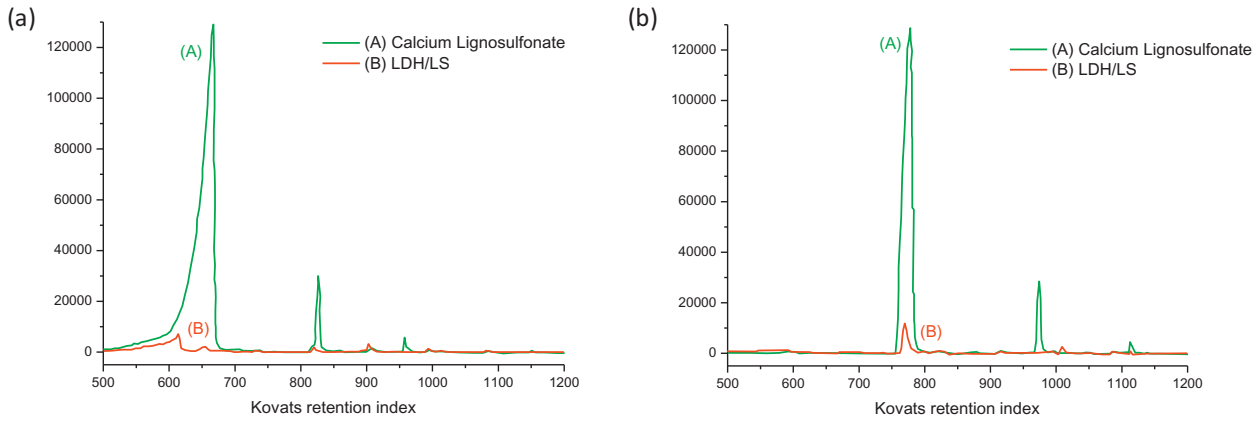

Fig. 1. Chromatographs obtained by electronic nose analysis of LS (A – green) and LDH/LS compounds (B – red) with column DB-5 (a) and DB-1701 (b). (For interpretation of the references to colour in this figure legend, the reader is referred to the web version of this article.)

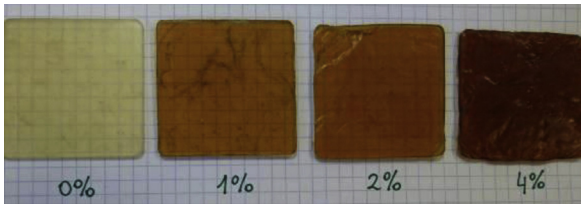

Fig. 2. Optical aspects of nanocomposites films (50 mm × 50 mm × 2 mm) prepared by compression moulding.

This can be understood considering that the shear applied in an internal mixer can orient individual nanofillers but may not orient large stack of layers (Chivrac et al., 2008). This may explain that the torque is nearly independent on LDH/LS concentration provided that an exfoliated state is reached. Mixtures had a brown colour due to the addition of LDH/LS particles but they were transparent at all filler content except the highest one (4 wt%) (Fig. 2). This result suggests the presence of well dispersed LDH/LS, very small particles within the starch matrix.

3.2.2. Characterization of the dispersion of LDH/LS in TCS by X-ray diffraction and transmission electron microscopy

50 mm × 50 mm × 2 mm samples were analyzed by X-ray diffraction to evaluate the level of intercalation or exfoliation of LDH/LS within the thermoplastic starch matrix. Fig. 3 shows the diffraction pattern of LDH/LS nanofillers, thermoplastic starch matrix and their nanocomposites with 1 and 4 wt% loadings.

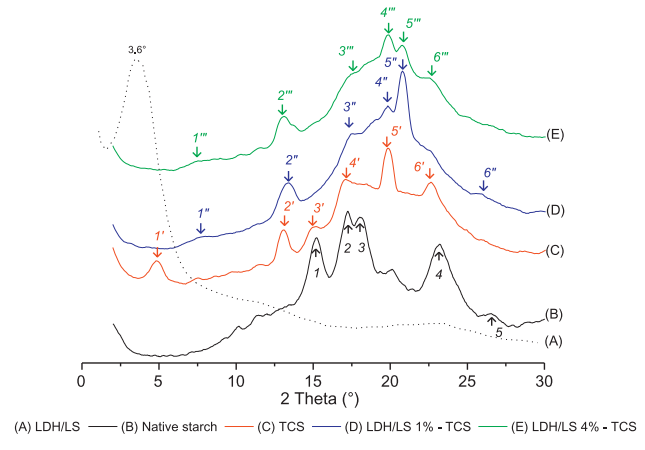

Fig. 3. X-ray diffraction patterns of (A) LDH/LS, (B) native starch, (C) thermoplastic corn starch, (D) thermoplastic corn starch, with 1 wt% LDH/LS and (E) thermoplastic corn starch with 4 wt% LDH/LS.

The diffraction peak at 3.6° for the pure LDH/LS corresponds to an interlayer distance of 2.4 nm (calculate by Bragg's law $2d\sin(\theta) = n\lambda$). This value is in the range of thickness of lignosulfonate molecules (1.5–2.1 nm) (Goring, Vuong, Gancet, & Chanzy, 1979), thus indicating a monolayer arrangement of LS inside LDH galleries. Fig. 3 shows that no diffraction peak is observed with the LDH/LS-filled TCS. This can be due to two reasons. Either nanofillers are well dispersed in an exfoliated state or the nanofiller concentration (1–4 wt%) is too low to generate a measurable signal. As will be seen later by TEM, LDH/LS is well exfoliated. Lignosulfonate is known to strongly interact with a starch phase (Baumberger, Lapierre, Monties, Lourdin, & Colonna, 1997; Morais, Curvelo, & Zambon, 2005), and such strong interactions may help the destacking of layer assembly, leading to an exfoliated structure. The incorporation of nanofillers into thermoplastics is usually changing the crystallization behaviour of the material (Huang, Yu, & Ma, 2004). In our case, crystallinity is slightly reduced by the addition of LDH/LS, from 12% for pure TCS to 10% for LDH/LS 1%–TCS and to 9% for LDH/LS 4%–TCS.

Starch has three main crystalline allomorphs called A, B and V. The A and B structures have a double helical structure with six glucose units per turn, with the A type having a monoclinic unit cell while the B type has a hexagonal unit (Imberty, Buléon, Tran, & Pérez, 1991). Cereal starch displays the A type while tuber starch is of the B type. Having corn starch, we should expect to have the A type in the native state, which is confirmed by the presence of characteristic peaks at 14.8°, 16.8°, 17.8°, 23° and 26.4° (Fig. 3 – curve B). The V type is itself composed of many allomorphs, presenting single left handed helices. It is mostly found after gelatinization or destructuration leading to thermoplastic starch and is the sign of a rearrangement of both amylose and amylopectine, called retrogradation. It has been observed that glycerol plasticized amylose-rich materials retrograde in B and V type mixtures (Myllarinen, Buléon, Lahtinen, & Forssell, 2002). We observed theses changes in our samples. While pure TCS is a mixture of B and Vh crystalline structures, a commonly encountered situation, the TCS with 1 wt% LDH/LS has only a Va structure while the loading with 4 wt% is a mix of Vh and Va structures (Table 3).

Transmission electron microscopy images show a uniform dispersion of LDH/LS nanofillers within the thermoplastic starch matrix for all filler contents. Dimension of the LDH/LS particles was about 70 nm length and ~3 nm thick corresponding to the LDH/LS interlayer (Fig. 4), showing an exfoliated state. The platelet particles have an aspect ratio (lateral dimension over thickness) larger than 20.

Table 3
Diffraction peak allocation of TCS and TCS filled with LDH/LS.

	Melt-blended		Literature[a]		
	No. figure 3	2θ angle (°)	2θ angle (°)	Intensity	Structure type
TCS	1	4,9	5.5	Medium	B
	2	13.1	13.3	Strong	Vh
	3	15	14.9	Weak	
	4	17	17	Medium	
	5	19.9	19.8	Very strong	
	6	22.6	22.6	Medium	
LDH/LS 1%–TCS	1′	7.9	7.9	Strong	Va
	2′	13.5	13.4	Very strong	
	3′	17.1	17.5	Medium	
	4′	19.9	19.4	Medium	
	5′	20.8	20.8	Very strong	
	6′	25.8	26.3	Weak	
LDH/LS 4%–TCS	1″	8.3	7.9	Strong	Va
	2″	13.1	13.4	Very strong	Vh,
	3″	17.4	17.5	Medium	Va
	4″	19.9	19.8	Very strong	Vh
	5″	20.7	20.8	Very strong	Va
	6″	22.6	22.6	Medium	Vh

[a] Van Soest, Hulleman, and Vliegenthart (1996).

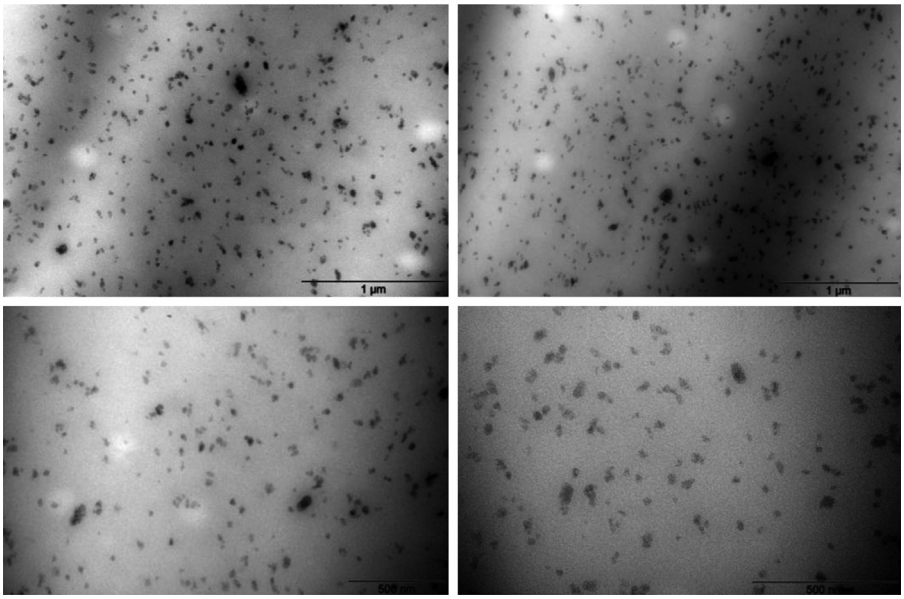

Fig. 4. Transmission electron microscopy images of thermoplastic corn starch mixtures containing 1 wt% of LDH/LS at different magnifications.

3.2.3. *Mechanical properties of TCS and LDH/LS–TCS nanocomposites*

Table 4 gives the tensile properties (Young's modulus, tensile strength and elongation at break) for thermoplastic corn starch (TCS) and LDH/LS–TCS nanocomposites after two weeks of stabilization at 20 °C and 55% RH. The main results are that starch with 1 wt% LDH/LS shows an interesting property improvement while higher LDH/LS concentrations exhibit degraded properties. An increase of stiffness is observed with 1 wt% LDH/LS loading with a 30% improvement, but a decrease of stiffness to low values at 2 and 4 wt% loading. The stress at break follows the same trend with filler content where 1 wt% LDH/LS nanocomposite has a value slightly larger than the one of thermoplastic corn starch (TCS) but a strong decrease is observed at higher filler concentration. Similar results were reported in literature for starch filled with LDH where the stress at break increases when a low level of LDH loading around 3 wt% is reached (Chung & Lai, 2010; Wu et al., 2011). Elongations at break are increased with LDH/LS loading whatever the loading level is. No variation of elongation at break with concentration is observed in case of exfoliated nanocomposites (Chivrac et al., 2008), which is not the case here. One reason could be that the addition of hydrophilic nanofiller able to build strong polar interactions with water may help to retain water molecules, leading to a more plasticized material. Lignosulfonate is already known to plasticize starch material (Baumberger et al., 1997).

Table 4
Tensile properties of TCS and LDH/LS–TCS nanocomposite.

	Young's modulus (MPa)	Stress at break (MPa)	Elongation at break (%)
TCS	7.3 (1.0)	2.7 (0.2)	61 (5)
LDH/LS 1%–TCS	10.2 (2.3)	3.2 (0.1)	100 (7)
LDH/LS 2%–TCS	2.3 (0.4)	1.7 (0.1)	101 (2)
LDH/LS 4%–TCS	1.5 (0.1)	1.4 (0.1)	104 (6)

Mean value (standard deviation).

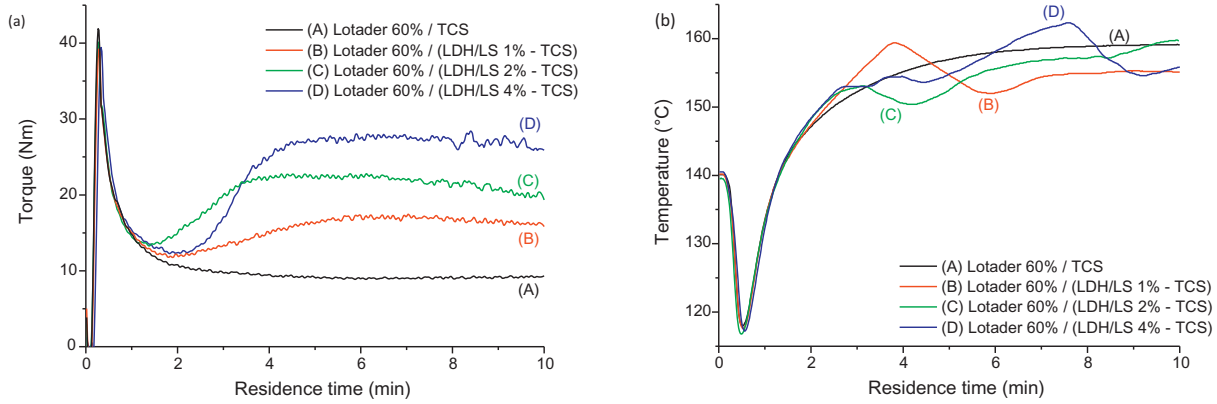

Fig. 5. Torque (a) and temperature (b) as a function of residence time during the mixing of Lotader 60%/TCS and Lotader 60%/TCS filled with LDH/LS (1, 2 and 4 wt%).

After melt processing, thermoplastic starch undergoes retrogradation which provides crystallization and reduces the elongation at break (Van Soest, Hulleman, De Wit, & Vliegenthart, 1996; Van Soest, Hulleman, & Vliegenthart, 1996). Introduction of nanofillers may stop or reduce this re-crystallization process, a phenomenon already observed with starch–clay nanocomposite (Magalhães & Andrade, 2009).

A large contribution of mechanical improvement is due to the quality of the interfacial contact between fillers and the matrix at a nanoscale level and to the overall morphology. The best compromise seems to be achieved for 1 wt% loading compare to 2 and 4 wt%, resulting to a mechanical improvement of starch based nanocomposite only for the 1 wt% loading.

3.3. Thermoplastic/(LDH/LS–TCS) composite

Lignosulfonates, as most lignin-based compounds, starts to degrade at temperatures above 200 °C, much higher than the processing temperature used during composite preparation (maximum temperature 140 °C).

3.3.1. Mixing process

The LDH/LS based-starch nanocomposites with 1, 2 and 4 wt% LDH/LS were blended with a thermoplastic matrix, Lotader 3210. This polyethylene matrix grafted with maleic anhydride was selected because of the presence of anhydride maleic which should facilitate adhesion between the two polymers by compatibilizing the interface through a chemical reaction between the hydroxyl groups present in starch molecules and the anhydride groups (Liu, Wang, & Sun, 2003). Fig. 5 shows the evolution of the torque and temperature with residence time in the internal mixer during melt processing. Temperature was regulated during processing in order to keep the blend temperature under 160 °C for avoiding starch degradation. Mixing time was also limited to 10 min for the same reason. After a first sharp increase of torque corresponding to the introduction of the two components in the mixer chamber, torque decreases due to the melting of the thermoplastic polymer. Without starch, this torque is then constant with time. When LDH/LS–TCS is present, the torque increase is interpreted as the dispersion and distribution of LDH/LS–TCS in the molten thermoplastic polymer. This process takes about two minutes after which the torque is nearly constant with time. However, in some cases, a small decrease of torque with time is seen, as a sign of a slight degradation of starch (as evidenced on C, Fig. 5a).

The final torque value increases with LDH/LS nanofiller concentration as expected, since viscosity of the LDH/LS-filled thermoplastic starch is increasing with filler concentration. All formulations have a homogeneous visual aspect from cream-white to brown colour.

3.3.2. Mechanical properties of thermoplastic/(LDH/LS–TCS) blends

The tensile properties of four samples were measured after storage in a conditioning room (20 °C–55% RH). Table 5 shows the tensile properties obtained for Lotader/(LDH/LS–TCS) with two

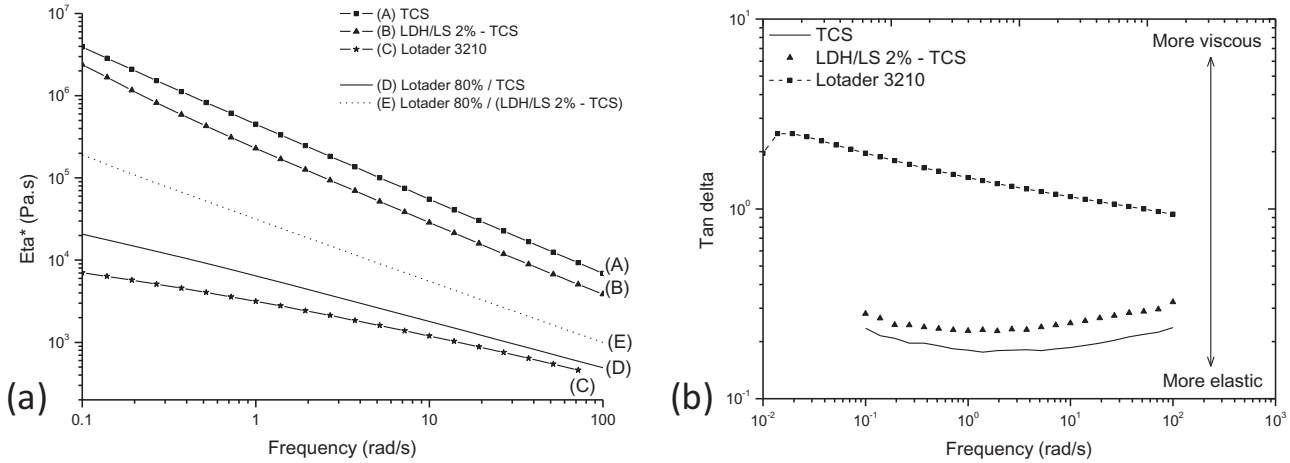

Fig. 6. Viscosity (a) and tan δ (b) versus frequency of (A) TCS, (B) TCS–LDH/LS 2%–TCS, (C) Lotader 3210 and their blends, (D) Lotader 80%/TCS and (E) Lotader 80%/(LDH/LS 2%–TCS).

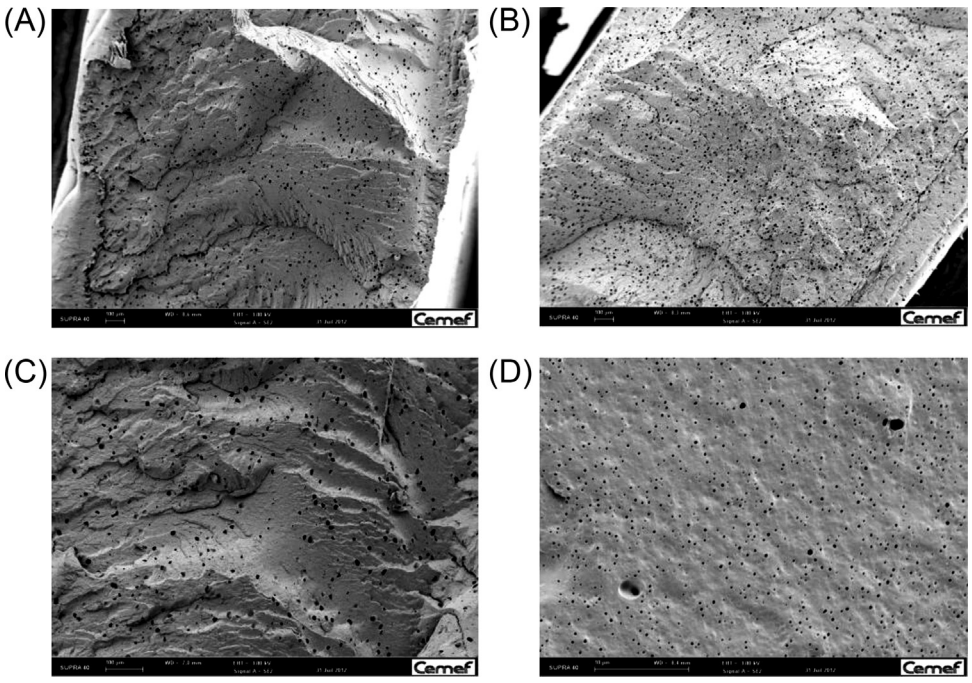

Fig. 7. Scanning electron micrographs of Lotader 80%/TCS (a), Lotader 60%/TCS (b), and Lotader 80%/(LDH/LS 1%–TCS) (c), and Lotader 60%/(LDH/LS 2%–TCS) (d).

composition ratios 80/20 and 60/40 by weight, the properties for pure Lotader and unfilled TCS being reported for comparison.

The addition of 20 wt% of TCS into a Lotader matrix decreases the mechanical properties. Surprisingly, a Young's modulus close to the pure Lotader was recorded with 40 wt% starch replacement, while strength and elongation at break were strongly decreased. Table 5 shows that the most interesting blends are with 20 wt% of starch-based content. Whatever the LDH/LS loadings into TCS are, the mechanical properties of the blends with Lotader are in the range of pure Lotader. A clear reinforcement is already observed at LDH/LS content as small as 1 wt% into starch. Tensile strength is around 76.9 MPa for Lotader/(LDH/LS 1%–TCS), much higher than for Lotader/TCS (38.7 MPa). Tensile strength and elongation at break for Lotader 80%/(LDH/LS–TCS) are similar to pure Lotader. Improvement in tensile strength can be attributed to the formation of a three-dimensional network reinforcing the blend through a percolation mechanism (Raquez, Nabar, Narayan, & Dubois, 2011). LDH contents of 2 and 4 wt% are not presenting any advantage compared to content of 1 wt%, somehow in slight discrepancy with an usually reported optimal loading of around 3 wt%. Classically, the non exfoliated nanofiller fraction increases with filling content, forming large aggregates and leading to more brittleness of nanocomposites (Alexandre & Dubois, 2000). A similar trend is obtained for the blends using 40% starch-based fraction.

3.3.3. *Rheological properties of thermoplastic/(LDH/LS–TCS) blend*

Morphology development in incompatible polymer blends is a function of stress, strain, flow type, interfacial tension, and viscosity and elasticity ratios between both phases. Therefore rheology is a marker of both morphology and interactions between phases. TCS and LDH/LS–TCS composites and their blends with Lotader were studied in order to correlate the rheological properties with the mechanical results described above. Fig. 9 shows the dynamic viscosity of pure TCS, LDH/LS 2%–TCS, pure Lotader, Lotader 80%/TCS blend and Lotader 80%/(LDH/LS 2%–TCS) blend. TCS behaves like a jelly materials under test conditions, with a linear viscosity–frequency curve adopting a slope of −1 and low tangent delta (G' much higher than G''). Lotader is a classical viscoelastic polymer. Mixing with 2% of LDH/LS slightly decreases the strength of the TCS gel while on the contrary it increases the viscosity of Lotader. The interesting point is that the addition of starch filled with LDH/LS strongly increases the viscosity of Lotader, much more than the addition of unloaded pure thermoplastic starch. This

Table 5
Tensile properties of Lotader, TCS and Lotader/TCS with 0, 1, 2 and 4 wt% LDH/LS materials.

	Young's modulus (MPa)	Tensile strength (MPa)	Elongation at break (%)
References			
Lotader 3210	41.3 (1.8)	80.0 (2.8)	229 (3)
TCS	7.3 (1.0)	2.7 (0.2)	61 (5)
80/20			
Lotader/TCS	27.5 (0.5)	38.7 (4.8)	183 (11)
Lotader/(LDH/LS 1%–TCS)	31.5 (0.8)	76.9 (7.6)	221 (7)
Lotader/(LDH/LS 2%–TCS)	32.1 (1.4)	77.6 (9.3)	214 (8)
Lotader/(LDH/LS 4%–TCS)	32.3 (1.3)	74.3 (8.2)	202 (8)
60/40			
Lotader/TCS	45.5 (2.7)	16.8 (0.9)	91 (8)
Lotader/(LDH/LS 1%–TCS)	38.9 (1.2)	20.6 (2.8)	106 (13)
Lotader/(LDH/LS 2%–TCS)	39.3 (1.6)	21.2 (8.1)	104 (32)
Lotader/(LDH/LS 4%–TCS)	42.1 (3.4)	24.4 (4.8)	112 (14)

Mean value (standard deviation).

suggests that LDH/LS is interacting with Lotader. As a matter of fact, LDH/LS affects strongly the interactions between the constituents of Lotader/(LDH/LS–starch) blends as observed both by rheology and mechanical analysis.

The viscosity ratio measured in oscillatory mode are very high, about 23 for Lotader 80%/TCS blends and 12 for Lotader 80%/(LDH/LS 2%–TCS) blends (at 50 s^{-1}) (Fig. 6). This should not allow any breakage of drops and thus any refining of the blend morphology under shear since viscosity ratios larger than four do not permit drop deformation and break-up for Newtonian materials (Grace, 1982). However, as said, such data are not fully representative of the viscosity developed inside the mixer under large deformations.

3.3.4. Morphologies of Lotader/(LDH/LS–TCS) blends

As shown on Fig. 7, a uniform dispersion of LDH/LS particles in the thermoplastic starch matrix is observed for all filler contents, with dimension of the LDH/LS particles of about 70 nm length and ~3 nm thick.

In the Lotader/starch blends, the major component Lotader is the matrix and TCS is the dispersed phase. The morphology is a fine and homogeneous dispersion of starch particles with diameters below 0.5 μm. Such a low diameter range for dispersed phase is in large part due to the presence of anhydride maleic, which permits to decrease the interfacial tension between hydrophilic starch dispersed phase and the hydrophobic polyethylene part of Lotader matrix.

The analysis of SEM pictures shows that the mean diameter of the starch inclusions in Lotader/starch blends containing 20 wt% (Fig. 8, curve A) and 40 wt% (Fig. 8, curve B) of starch, were 0.3 μm and 0.5 μm respectively, consistent with literature data (Bastioli et al., 1997) and in agreement with the fact that increasing starch content increases the size of the dispersed phase (Bikiaris & Panayiotou, 1998).

TCS (Fig. 8, curve A) and LDH/LS 1%–TCS nanocomposite (Fig. 8, curve C) have nearly the same mean diameter of inclusions, around 0.3 μm. When the LDH/LS content increases, the mean diameter is reduced down to about 0.2 μm for LDH/LS 2%–TCS (Fig. 8 curve D) and LDH/LS 4%–TCS (Fig. 8, curve E).

3.3.5. Sensitivity to water and O_2

Water solubility is an important property in the field of packaging. Most of the time, packaging requires water insolubility to prevent product degradation, but at the same time, it requires having good oxygen barrier properties.

Cumulative water intakes of pure Lotader and 80% Lotader/TCS blend after 310 h are respectively 0.4% and 2.5%, this last value

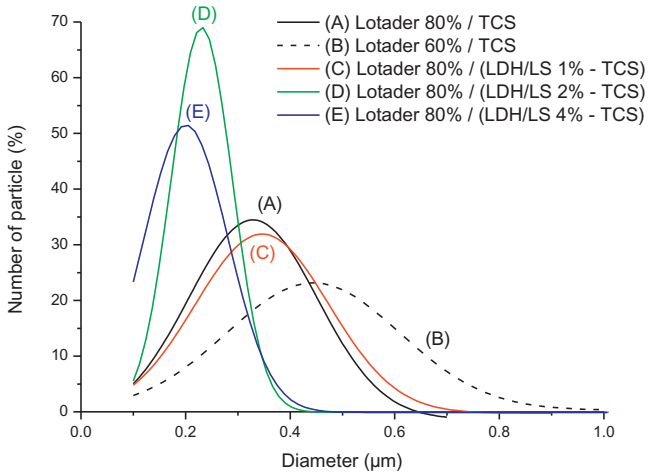

Fig. 8. Distribution of the diameter of the dispersed starch phase into the Lotader matrix for Lotader 80%/TCS (A), Lotader 60%/TCS (B), Lotader 80%/(LDH/LS 1%–TCS) (C), Lotader 80%/(LDH/LS 2%–TCS) (D), and Lotader 80%/(LDH/LS 4%–TCS) (E).

being due to the hydrophilic character of the starch phase. As far as water intake is concerned, blends prepared with a concentration of 20 wt% of LDH/LS–TCS have the same water intake than Lotader/TCS blends (Fig. 9b). For a starch phase content of 40 wt%, the addition of layered double hydroxides decreases by a factor of five the water diffusion coefficient and by half the maximum water intake after 310 h.

From 1 to 4 wt%, the blends absorb less water as the concentration of the filler increases. In Lotader/starch blends, the phase responsible to water sensitivity is starch which is very hygroscopic. LDH/LS nanofillers probably form hydrogen bonds with starch which may reduce the amount of hydroxyl groups accessible to water molecules. Similar results have been reported with starch nanocomposites prepared with montmorillonite or kaolin (Carvalho et al., 2001; Huang et al., 2004).

In spite of the hydrophilicity of the layered double hydroxide/lignosulfonate fillers, the equilibrium moisture uptake was found to decrease with the addition of LDH/LS compare to the neat Lotader/TCS blend. Such a result could be due to the morphology of nanocomposite. Addition of nanofillers creates a tortuous path which decreases the diffusion coefficient (Fig. 9a) (Cyras, Manfredi, Ton-That, & Vázquez, 2008).

Oxygen transmission rate was measured on blend and on their nanocomposites. First, the influence of TCS content in Lotader was studied (Fig. 10a). The increase of starch phase (from 20 to 40 wt%)

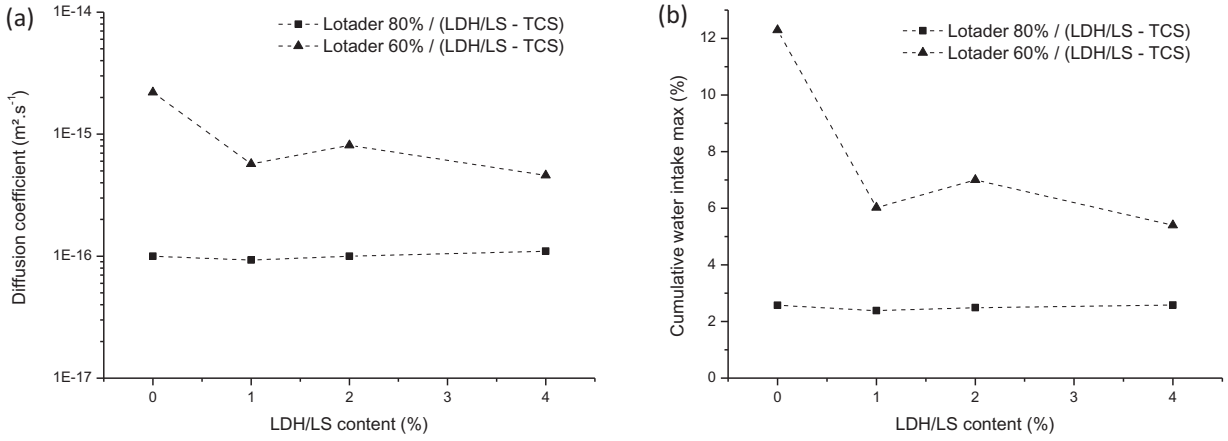

Fig. 9. Water diffusion coefficient (a) and equilibrium water intake (b) of Lotader/starch blends as a function of LDH/LS fillers content.

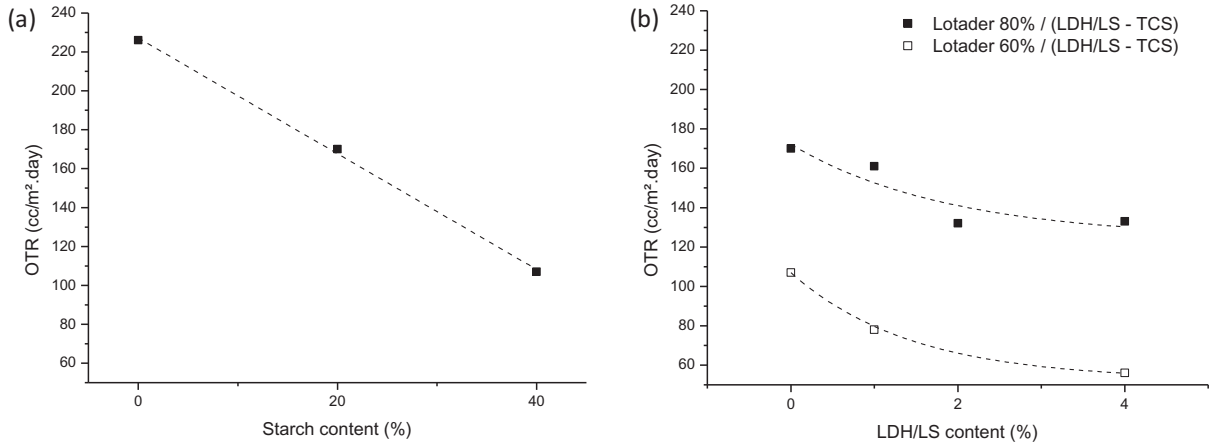

Fig. 10. Oxygen transmission rate for Lotader/TCS blend (a) and their nanocomposites filled with LDH/LS (b).

decreases drastically the oxygen transmission rate of the blend. It is already well know that thermoplastic starch has a low oxygen transmission rate (~150 $cm^3/(m^2\ day)$) compared to polyethylene (LDPE ~10,000 $cm^3/(m^2\ day)$), which is the main component of Lotader. The addition of LDH/LS decreases further the oxygen transmission rate, probably due to the tortuous platelet topology already advocated for the better resistance to water intake.

4. Conclusions

The incorporation of layered double hydroxide organo-modified by lignosulfonate (LDH/LS) into thermoplastic starch is an easy and straightforward process, resulting in a homogeneous dispersion of the LDH at the nanoscale range and reaching a nearly complete exfoliation. The use of LDH in a slurry form during preparation avoids the formation of LDH aggregates. The odour characteristic of lignosulfonate is largely attenuated due to the preparation process of these LDH. When thermoplastic starch is filled with a small amount of LDH/LS, as low as 1 wt%, a significant change of mechanical properties occurs, as well as an increase of oxygen and water barrier properties. This is a remarkable effect with expends the possibilities to use such reinforced thermoplastic starch as a filler in polymer composites. This was illustrated by preparing composites with 20 wt% of LDH/LS–TCS in a polyolefin matrix. Despite the addition of starch, the composite has mechanical properties close to the ones of the pure polyolefine matrix while improving oxygen barrier properties.

Acknowledgements

The work was performed in the frame of the Industrial Chair in Bioplastics supported by Arkema, L'Oréal, Nestlé, PSA Peugeot-Citroën and Schneider Electric. The authors thank Tembec and Arkema for providing materials, Alpha MOS for the odour analyses, Nestlé for O_2 permeability and Sophie Pagnotta (CCMA, Nice) for the TEM observations.

References

Alexandre, M., & Dubois, P. (2000). Polymer-layered silicate nanocomposites: Preparation, properties and uses of a new class of materials. *Materials Science and Engineering*, *28*, 1–63.

Armentano, I., Dottori, M., Fortunati, E., Mattioli, S., & Kenny, J. M. (2010). Biodegradable polymer matrix nanocomposites for tissue engineering: A review. *Polymer Degradation and Stability*, *95*, 2126–2146.

Bagdi, K., Muller, P., & Pukanszky, B. (2006). Thermoplastic starch/layered silicate composites: Structure, intercalation, properties. *Composite Interfaces*, *13*, 1–17.

Bastioli, C. (1998). Properties and applications of Mater-Bi starch-based materials. *Polymer Degradation and Stability*, *59*, 263–272.

Bastioli, C., Bellotti, V., Cella, G. D., Del Giudice, L., Montino, S., & Perego, G. (1997). Biodegradable polymeric compositions comprising starch and a thermoplastic polymer. European Patent EP 0 937 120 B1.

Baumberger, S., Lapierre, C., Monties, B., Lourdin, D., & Colonna, P. (1997). Preparation and properties of thermally moulded and cast lignosulfonates–starch blends. *Industrial Crops and Products*, *6*, 253–258.

Bikiaris, D., & Panayiotou, C. (1998). LDPE/starch blends compatibilized with PE-g-MA copolymers. *Journal of Applied Polymer Science*, *70*, 1503–1521.

Carvalho, A. J. F. de., Curvelo, A. A. S., & Agnelli, J. A. M. (2001). A first insight on composite of thermoplastic starch kaolin. *Carbohydrate Polymers*, *45*, 189–194.

Chaléat, C. M., Halley, P. J., & Truss, R. W. (2008). Properties of a plasticized starch blend. Part 1. Influence of moisture content on fracture properties. *Carbohydrate Polymers*, *71*, 535–543.

Chen, B. Q., & Evans, J. R. G. (2005). Thermoplastic starch–clay nanocomposites and their characteristics. *Carbohydrate Polymers*, *61*, 455–463.

Chiou, B. S., Yee, E., Wood, D., Shey, J., Glenn, G., & Orts, W. (2006). Effects of processing conditions on nanoclay dispersion in starch–clay nanocomposites. *Cereal Chemistry*, *83*, 300–305.

Chivrac, F., Kadlecova, Z., Pollet, E., & Avérous, L. (2006). Aromatic copolyester-based nanobiocomposites: Elaboration, structural characterization and properties. *Journal of Polymers and the Environment*, *14*, 393–401.

Chivrac, F., Pollet, E., Schmutz, M., & Avérous, L. (2008). New approach to elaborate exfoliated starch-based nanobiocomposites. *Biomacromolecules*, *9*, 896–900.

Chung, Y.-L., & Lai, H.-M. (2010). Preparation and properties of biodegradable starch-layered double hydroxide nanocomposites. *Carbohydrate Polymers*, *80*, 525–532.

Costantino, U., Nocchetti, M., Tammaro, L., & Vittoria, V. (2012). Modified hydrotalcite-like compounds as active fillers of biodegradable polymers for drug release and food packaging applications. *Recent Patents on Nanotechnology*, *6*, 218–230.

Cyras, V. P., Manfredi, L. B., Ton-That, M-T., & Vázquez, A. (2008). Physical and mechanical properties of thermoplastic starch/montmorillonite nanocomposite films. *Carbohydrate Polymers*, *73*, 55–63.

Dufresne, A., Dupeyre, D., & Vignon, M. (2000). Cellulose microfibrils from potato tuber cells: Processing and characterization of starch–cellulose microfibril composites. *Journal of Polymer Science*, *76*, 2080.

Follain, N., Joly, C., Dole, P., & Bliard, C. (2005). Mechanical properties of starch-based materials. I. Short review and complementary experimental analysis. *Journal of Applied Polymer Science*, *97*, 1783–1794.

Forssell, P. M., Mikkilä, J. M., Moates, G. K., & Parker, R. (1997). Phase and glass transition behaviour of concentrated barley starch–glycerol–water mixtures, a model for thermoplastic starch. *Carbohydrate Polymers*, *34*(4), 275–282.

Goring, D. A. I., Vuong, R., Gancet, C., & Chanzy, H. (1979). The flatness of lignosulfonate macromolecules as demonstrated by electron microscopy. *Journal of Applied Polymer Science*, *24*, 931–936.

Grace, H. P. (1982). Dispersion phenomena in high-viscosity immiscible fluid systems and application of static mixers as dispersion devices in such systems. *Chemical Engineering Communications*, *14*, 225–277.

Hennous, M., Derriche, Z., Privas, E., Navard, P., Verney, V., & Leroux, F. (2013). Lignosulfonate interleaved layered double hydroxide: A novel green organoclay for bio-related polymer. *Applied Clay Science*, *71*, 42–48.

Hermans, P. H., & Weidinger, A. (1949). X-ray studies on the crystallinity of cellulose. *Journal of Polymer Science*, *4*, 135–144.

Huang, M-F., Yu, J-G., & Ma, X-F. (2004). Studies on the properties of montmorillonite–reinforced thermoplastic starch composites. *Polymer*, *45*, 7017–7023.

Imberty, A., Buléon, A., Tran, V., & Pérez, S. (1991). Recent advances in knowledge of starch structure. *Starch/Stärke*, *43*, 375–384.

Leroux, F. (2006). Organo-modified anionic clays into polymer compared to smectite-type nanofiller: Potential applications of the nanocomposites. *Journal of Nanoscience and Nanotechnology*, *6*, 303–315.

Leroux, F., Chabrol, K., Morlat-Thérias, S., Gardette, J. L., & de Roy, A. (2012). Formation of single-layered double-hydroxide platelets in poly(vinylpyrrolidone) and alginate medium: Conductive, capacitive, and dielectric properties of the hybrid films. *European Journal of Inorganic Chemistry*, *32*, 5332–5342.

Liu, W., Wang, Y-J., & Sun, Z. (2003). Effects of polyethylene-grafted maleic anhydride (PE-g-MA) on thermal properties, morphology and tensile properties of low-density polyethylene (LDPE) and corn starch blends. *Journal of Applied Polymer Science*, *88*, 2904–2911.

Magalhães, N. F., & Andrade, C. T. (2009). Thermoplastic corn starch/clay hybrids: Effect of clay type and content on physical properties. *Carbohydrate Polymers*, *75*, 712–718.

Morais, L. C., Curvelo, A. A. S., & Zambon, M. D. (2005). Thermoplastic starch–lignosulfonate blends. 1. Factorial planning as a tool for elucidating new data from high performance size-exclusion chromatography and mechanical tests. *Carbohydrate Polymers*, *62*, 104–112.

Myllarinen, P., Buléon, A., Lahtinen, R., & Forssell, P. (2002). The crystallinity of amylose and amylopectine films. *Carbohydrate Polymers*, *48*, 41–48.

Nguyen, T.-P. (2011). Polymer-based nanocomposites for organic optoelectronic devices: A review. *Surface and Coatings Technology*, *206*, 742–752.

Oh, J. M., Park, D. H., Choi, S. J., & Choy, J. H. (2012). LDH nanocontainers as bio-reservoirs and drug delivery carriers. *Recent Patents on Nanotechnology*, *6*, 200–217.

Pandey, J. K., & Singh, R. P. (2005). Green nanocomposites from renewable resources: Effect of plasticizer on the structure and material properties of clay-filled starch. *Starch/Stärke*, *57*, 8–15.

Park, H. M., Lee, W. K., Park, C. Y., Cho, W. J., & Ha, C. S. (2003). Environmentally friendly polymer hybrids. Part I. Mechanical, thermal and barrier properties of thermoplastic starch/clay nanocomposites. *Journal of Materials Science*, *38*, 909–915.

Park, H. M., Li, X. C., Jin, C. Z., Park, C. Y., Cho, W. J., & Ha, C. S. (2002). Preparation and properties of biodegradable thermoplastic starch/clay hybrids. *Macromolecular Materials and Engineering*, *287*, 553–558.

Peters, J., Fischer, K., & Fischer, S. (2008). Characterization of emissions from thermally modified wood and their reduction by chemical treatment. *BioResources*, *3*(2), 491–502.

Raquez, J-M., Nabar, Y., Narayan, R., & Dubois, P. (2011). Preparation and characterization of maleated thermoplastic starch-based nanocomposites. *Journal of Applied Polymer Science*, *122*, 639–647.

Sanchez-Paniaguar Lopez, M., Leroux, F., & Mousty, C. (2010). Amperometric biosensor based on hybrid LDH–alginate nanocomposite for aqueous and non aqueous detection of phenolic compounds. *Sensors and Actuators B: Chemical*, *150*, 36–42.

Tang, X. Z., Kumar, P., Alavi, S., & Sandeep, K. P. (2012). Recent advances in biopolymers and biopolymer-based nanocomposites for food packaging materials. *Critical Reviews in Food Science and Nutrition*, *52*, 426–442.

Utracki, L. A., Sepehr, M., & Boccaleri, E. (2007). Synthetic, layered nanoparticles for polymeric nanocomposites (PCNs). *Polymers for Advanced Technologies*, *18*, 1–37.

Vaia, R. A., & Giannelis, E. P. (1997). Lattice model of polymer melt intercalation in organically modified layered silicates. *Macromolecules*, *30*, 7990–7999.

Van Soest, J. J. G., & Esser, P. J. (1997). Influence of amylose–amylopectin ratio on properties of extruded starch plastic sheets. *Journal of Macromolecular Science: Pure and Applied Chemistry Supplement*, *34*, 1665–1689.

Van Soest, J. J. G., Hulleman, S. H. D., De Wit, D., & Vliegenthart, J. F. G. (1996). Changes in the mechanical properties of thermoplastic potato starch in relation with changes in B-type crystallinity. *Carbohydrate Polymers*, *39*, 225–232.

Van Soest, J. J. G., Hulleman, S. H. D., & Vliegenthart, J. F. G. (1996). Crystallinity in starch bioplastics. *Industrial Crops and Products*, *5*, 11–22.

Wihelm, H.-M., Sierakowski, M.-R., Souza, G. P., & Wypych, F. (2003a). The influence of layered compounds on the properties of starch/layered compound composites. *Polymer International*, *52*, 1035–1044.

Wihelm, H.-M., Sierakowski, M.-R., Souza, G. P., & Wypych, F. (2003b). Starch films reinforced with mineral clay. *Carbohydrate Polymers*, *52*, 101–110.

Wu, D., Chang, P. R., & Ma, X. (2011). Preparation and properties of layered double hydroxide-carboxymethylcellulose sodium/glycerol plasticized starch nanocomposites. *Carbohydrate Polymers*, *86*, 877–882.

Zhao, X., Lv, L., Pan, B., Zhang, W., Zhang, S., & Zhang, Q. (2011). Polymer supported nanocomposites for environmental application: A review. *Chemical Engineering Journal*, *170*, 381–394.